Measurement of Tibiofemoral Kinematics Using Highly Accelerated 3D Radial Sampling

Jarred Kaiser,[1] Robert Bradford,[1] Kevin Johnson,[2] Oliver Wieben,[2–4] and Darryl G. Thelen[1,4*]

This study investigated the use of dynamic, volumetric MRI to measure 3D skeletal motion. Ten healthy subjects were positioned on a MR-compatible knee loading device and instructed to harmonically flex and extend their knee at 0.5 Hz. The device induced active quadriceps loading with knee flexion, similar to the load acceptance phase of gait. Volumetric images were continuously acquired for 5 min using a 3D cine spoiled gradient-echo sequence in conjunction with vastly under-sampled isotropic projection reconstruction. Knee angle was simultaneously monitored and used retrospectively to sort images into 60 frames over the motion cycle. High-resolution static knee images were acquired and segmented to create subject-specific models of the femur and tibia. At each time frame, bone positions and orientations were determined by automatically registering the skeletal models to the dynamic images. Three-dimensional tibiofemoral translations and rotations were consistent across healthy subjects. Internal tibia rotations of $7.8 \pm 3.5°$ were present with $35.8 \pm 3.8°$ of knee flexion, a pattern consistent with knee kinematic measures during walking. We conclude that vastly under-sampled isotropic projection reconstruction imaging is a promising approach for noninvasively measuring 3D joint kinematics, which may be useful for assessing cartilage contact and investigating the causes and treatment of joint abnormalities. Magn Reson Med 000:000–000, 2012. © 2012 Wiley Periodicals, Inc.

Key words: dynamic imaging; knee mechanics; joint motion; VIPR

Magnetic resonance (MR) imaging is routinely used to identify structural damage (e.g., ligament tears and cartilage defects) and inflammation in musculoskeletal joints (1). However, imaging is normally performed in unloaded static postures, preventing insight into the function of joint tissues during normal movement (2). This is important to consider, because the causes and symptoms of musculoskeletal pathology are often linked to function.

[1]Department of Mechanical Engineering, University of Wisconsin-Madison, Madison, Wisconsin, USA.

[2]Department of Medical Physics, University of Wisconsin-Madison, Madison, Wisconsin, USA.

[3]Department of Radiology, University of Wisconsin-Madison, Madison, Wisconsin, USA.

[4]Department of Biomedical Engineering, University of Wisconsin-Madison, Madison, Wisconsin, USA.

*Correspondence to: Darryl G. Thelen, 1513 University Avenue, Madison, WI 53706. E-mail: thelen@engr.wisc.edu

For example, anterior knee pain can result from patellar maltracking that is only evident with active quadriceps loading (3,4). Further, abnormal knee kinematics in reconstructed knees may alter cartilage loading in a way that contributes to osteoarthritis risk (5).

Dynamic MR imaging is a powerful approach to measure functional in vivo joint motion (2), which can in turn be coupled with high-resolution musculoskeletal models to characterize joint rotation axes (6), lever arms of muscles (7), and cartilage contact (8). Prior MR studies have used real-time (3), cine phase contrast (PC; Ref. 9), and fast multiplanar (10) sequences to measure skeletal kinematics. Real-time imaging represents an ideal approach, but current temporal and spatial constraints only allow for a single planar image of relatively slow motion to be captured (3,11). Cine PC imaging has been used to measure three-dimensional tissue velocities, which are then integrated to estimate 3D skeletal motion (9,12,13). However, only a single cine PC image plane can be acquired in reasonable scan times, making it challenging to register absolute skeletal position and orientation in 3D space. In addition, numerical integration drift may contribute to errors at the position level. Dynamic anatomical scans of multiple, parallel planes provide 3D data to which high-resolution skeletal models can be registered (10). Again, only a few imaging planes can be captured in reasonable scan times, which likely limits the accuracy with which 3D orientation and position can be ascertained.

The purpose of this study was to investigate the feasibility of using a novel dynamic, volumetric MR imaging sequence to measure 3D skeletal motion at the knee. Volumetric imaging is achieved using radially under-sampled trajectories, termed vastly under-sampled isotropic projection (VIPR), which reduces scan time to a reasonable level while maintaining excellent resolution (14). In this study, we show that high-resolution skeletal models derived from static images can be registered to the volumetric VIPR images, thereby providing quantitative measures of skeletal position and orientation throughout a cyclic motion (Fig. 1). The relevance of such information for investigating in vivo joint mechanics and pathologies is discussed.

METHODS

Subjects

We collected images bilaterally on 10 healthy subjects (five females, five males, age: 24.6 ± 3.2 years; mass:
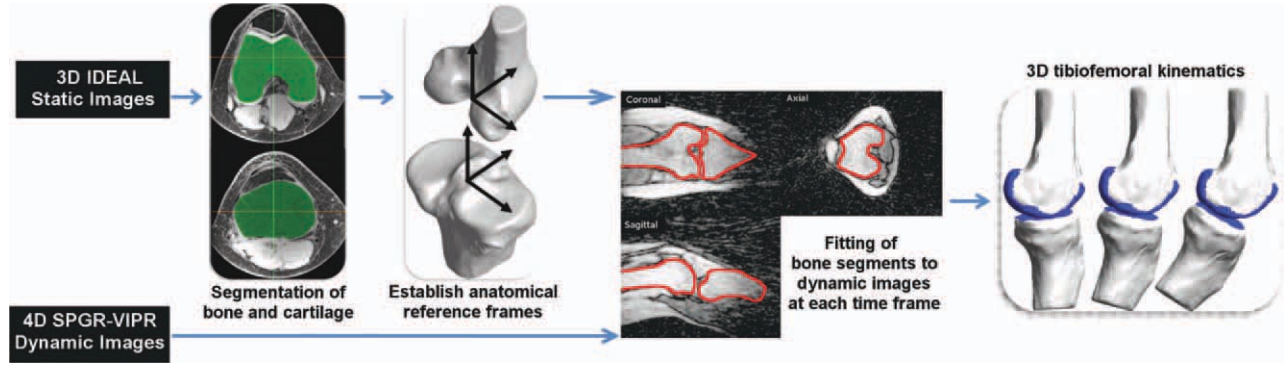
FIG. 1. Flow chart of dynamic imaging approach to track tibiofemoral kinematics. Volumetric models of the femur and tibia are segmented from static images, and then registered with dynamic SPGR-VIPR images at each frame of the motion. The final result is a 3D reconstruction of tibiofemoral kinematics.

65.1 ± 5.0 kg) who had no history of past knee injuries, pathologies, surgeries, or chronic knee pain. Informed consent was obtained prior to testing according to a protocol approved by the University of Wisconsin's Health Sciences Institutional Review Board.

Knee Flexion–Extension Task

Subjects were asked to perform a cyclic knee flexion–extension task. Subjects were positioned supine in a MR-compatible dynamic knee loading device (15), with the knee aligned to a leg brace rotation axis (Fig. 2). An inertial load was generated by a set of rotating disks that were geared to the knee rotation axis. The device induces quadriceps loading with knee flexion, as seen in the stance phase of gait (16,17).

The subjects first practiced the task in a laboratory, while external loading and knee motion were monitored to assess the biomechanics and repeatability of the task. Subjects were asked to flex and extend their knees at 0.5 Hz for 5 min. A semicircular structure was placed around the leg to mimic the bore size of the MR scanner used in this study. Applied load was measured at 1000 Hz using load cells embedded in the top and bottom belts (500 lb LCM-300, Futek, Irvine, CA). An MR-compatible rotary encoder (Micronor, Newbury Park, CA) placed on the knee axis shaft was used to monitor knee flexion angle at 50 Hz. Load and angle data were used together with an inverse dynamics analysis of the lower leg to ascertain the net internal knee extensor moment throughout the task.

MR Image Acquisition

The imaging session involved the acquisition of two volumetric data sets: (a) high-resolution static images that were segmented to obtain volumetric models of the femur and tibia and (b) lower-resolution dynamic images that were continuously acquired while the subject performed the cyclic movement within the bore of a scanner.

High-resolution static imaging of the subject's knee was performed using a 3D IDEAL spoiled gradient-echo (SPGR) sequence (512 × 512 × 304 cubic voxels with 0.37-mm spacing, 9-min scan) in a clinical 3.0-T MR scanner (MR750, General Electric Healthcare, Waukesha,

WI). For these scans, an eight-channel phased-array extremity coil (Precision Eight TX/pulse repetition time (TR) High Resolution Knee Array; Invivo, Orlando, FL) was positioned about the knee. The tibia and femur were manually segmented (MIMICS, Materialise Group, Leuven, Belgium) from the static images to create subject-specific bone models. The resulting models were smoothed (Geomagic, Research Triangle Park, NC) and decimated to ~15,000 vertices per bone. Local anatomical coordinate systems were separately established for the femur and tibia using a localization algorithm that establishes orthogonal anatomical axes for each bone based on geometric and inertial properties of the 3D segments (18). The repeatability and accuracy of this approach has been previously established for the knee (18).

Dynamic MR images of the knee were acquired while the subjects performed the cyclic, repeatable knee flexion–extension task within the bore of a scanner. A single channel General Purpose Flex Coil (General Electric Healthcare, Waukesha, WI) was attached to the loading device and held in a fixed position over the knee, with the coil parallel to the primary magnetic field. The subject was instructed to flex and extend their knee at 0.5 Hz for 5 min. Cadence was maintained via a metronome played over headphones. Volumetric images were
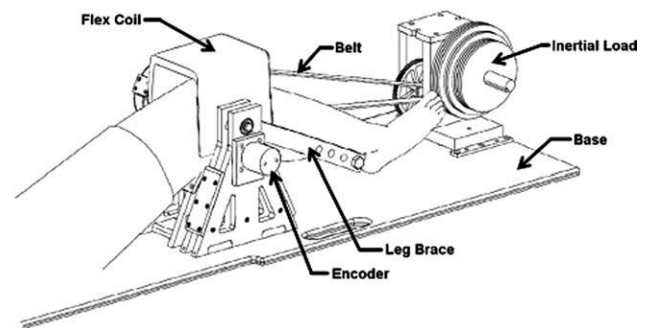

FIG. 2. Subjects performed cyclic knee flexion/extension in an MR-compatible loading device. A set of rotating inertial disks induce active quadriceps loading with knee flexion. A MR-compatible encoder is used to continuously measure knee angle throughout the dynamic imaging scan.
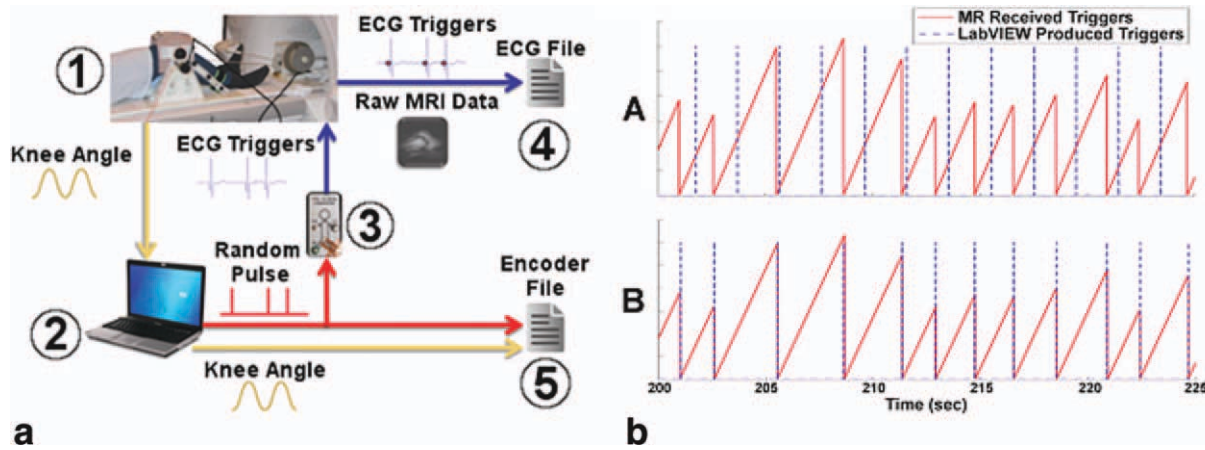
FIG. 3. **a:** Data acquisition during dynamic knee motion. Knee angle (1) is monitored in real-time (2). Simultaneously, a random pulse is generated and converted into an artificial ECG signal (3) that is monitored via the scanner (4). Generated pulse and knee angle are saved separate from MRI data (5). ECG triggers are subsequently used for retrospective alignment of the knee angle and image data. **b:** Unaligned (A) and aligned (B) triggers as recorded by the MR scanner and LabVIEW. The randomly spaced triggers were easily aligned in post hoc analysis, allowing for synchronization of the encoder and image information. [Color figure can be viewed in the online issue, which is available at wileyonlinelibrary.com.]

continuously acquired using a SPGR sequence in conjunction with VIPR (SPGR-VIPR). The order of the projection angles was determined with a pseudorandom 2D-bit reverse algorithm, which allows retrospective selection of projection numbers per time frame with an almost even distribution of angles. Relevant imaging parameters include: 1.5 mm isotropic acquired resolution, pulse repetition time/echo time = 4 ms/1.4 ms, flip angle = 8°, receiver bandwidth = 62.5 kHz, 75,000 unique radial lines, 48 cm field of view, scan time = 5 min.

Knee flexion angle was measured in the scanner via the MR-compatible rotary encoder mounted at the leg brace shaft. The encoder data were used to synchronize the image and motion data to allow for image reconstruction based on knee position. To do this, a LabVIEW (National Instruments, Austin, TX) program was used to monitor encoder counts at 50 Hz while generating randomly timed pulse triggers that were read into the scanner's cardiac gating system (Fig. 3). A custom MATLAB routine was used to retrospectively align the randomly generated triggers in LabVIEW with those measured by the MR gating module, allowing for both scaling corrections and a bulk time offset between the scanner-based and encoder-based times. Once aligned, the encoder data were interpolated to match the scanner-based time values, enabling the separation of all scanner-based data into position-based cycles. The beginning and end of each cycle was defined as the point at which the subject, during extension, reached the overall mean knee flexion angle. Then, a percent value was assigned to each projection based on when the projection was acquired in the flexion–extension cycle. Scanner matrix data were sorted by percent cycle, and a vector of the reordered projection reference numbers was output to a separate file.

Image reconstruction software reorganized the raw image data based on the reordered projections and binned the data into 60 equally sized 3D image frames.

Each frame represented an average of image data acquired during 1.67%, or 33 ms, of the 2 s flexion–extension cycle. Each 3D image was reconstructed utilizing a conjugate gradient least squares minimization (19). Unlike standard gridding reconstructions, this iterative technique did not require sampling density compensation, which is difficult to obtain for the irregularly spaced sampling present with retrospectively motion gating.

Registering Subject-Specific Bone Models

To establish a rough registration in the first 3D dynamic image frame, we first manually aligned anatomical landmarks that were visible in both the models and the image. We then used Powell's numerical optimization method (20) to align each bone segment to the dynamic image data at each time frame. This was done by finding the bone segment position and orientation that minimized the sum-squared intensities of the dynamic image at the locations of the model vertices. This routine drives the vertices of the bone segment models to the dark, low-intensity outlines of the bones in the dynamic images. The search region was bounded with a penalty function to prevent a solution in the low-intensity regions outside of the limb. The optimization solution for one frame was then used recursively as the initial guess for bone positions and orientations in the subsequent frame. This process was repeated for all 60 frames for each bone segment. The final result was a set of 3D translational and angle trajectories for the femur and tibia over the motion cycle. Kinematic trajectories were subsequently low-pass filtered with a 5 Hz cutoff frequency, which is 10 times higher than the nominal cycle rate. Knee angles were characterized by three successive body-fixed rotations that describe the orientation of the tibia relative to the femur (21).
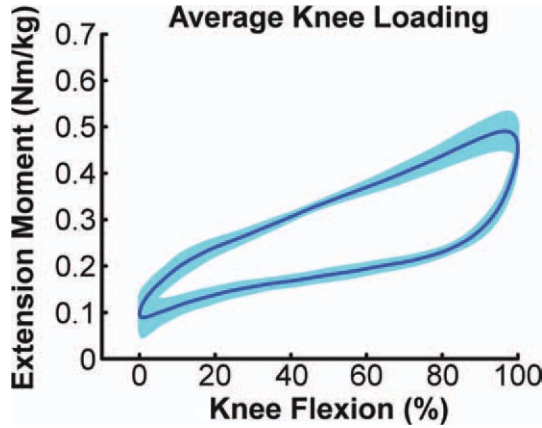
FIG. 4. Average (±1 standard deviation) knee extension moment induced over 150 consecutive knee flexion–extension motion cycles for one subject. Knee flexion is expressed as a percentage of the maximum flexion angle reached over the motion cycle.

Influence of Dynamic Image Reconstruction Parameters

We separately performed a sensitivity analysis to assess the effects of scan time and number of reconstructed frames on the measured knee kinematics. Shorter scan times were simulated by undersampling the full acquired data by factors of 2–4 to nominally represent information that would be obtained with scan times of 2.5, 1.67, and 1.25 min, respectively. Each cyclic image set was initially binned into 60 frames. We then assessed the effect of binning the full data of three subjects into 30, 45, and 75 frames. The root-mean-squared difference of kinematic measures from the nominal condition (5-min scan time, 60 frames) was used to quantify the effect of shorter scan times and different number of frames.

RESULTS

Repeatability

All subjects maintained a desired average cyclic motion period of 2.0 s, with standard deviations of less than 40 ms over 150 consecutive cycles. The range of knee flexion achieved in the scanner by the subjects was 35.8 ± 3.8°. For individual subjects, the peak knee flexion

and extension angles exhibited standard deviations of <0.7° over repeat cycles. The loading device induced maximum knee extension moments of ∼0.5 N m/kg, with peak loading coinciding with the knee flexion phase of the motion (Fig. 4).

Tibiofemoral Kinematics

The optimization routine produced bone positions and orientations that visually agree well with the dynamic image volumes (Fig. 5). The tibiofemoral kinematic trajectories were generally similar across knees, with all subjects exhibiting little frontal plane motion and internal tibia rotation with knee flexion (Fig. 6). The magnitude of internal tibia rotation averaged 7.8 ± 3.5° across subjects. The primary tibiofemoral translations were in the sagittal plane, with the tibia reference frame translating posterior and superior with knee flexion.

Dynamic Image Reconstruction

Varying the number of reconstruction frames between 30 and 75 had a relatively small effect on the knee kinematics obtained, with a maximum root-mean-squared difference of <1° in tibia angles over the motion cycle (Fig. 7). Reducing scan times had a greater effect on tibia rotation measures than adduction or flexion angles (Fig. 7). On average, changes in adduction and rotation angles varied 0.4 and 0.7° from the nominal case. Tibia translations remained within 0.75 mm root-mean-squared difference with the nominal case.

DISCUSSION

In this study, we have demonstrated the potential for using volumetric SPGR-VIPR imaging to track in vivo skeletal kinematics. A key to our approach is the use of radially under-sampled (VIPR) acquisitions, which allows one to obtain dynamic images with isotropic voxel resolution within a reasonable scan time. A second key was the simultaneous measurement of knee motion, which was used to retrospectively synchronize the dynamic images to the cyclic task. We showed that high-resolution bone models could be coregistered to the dynamic images, which allows for the quantitative
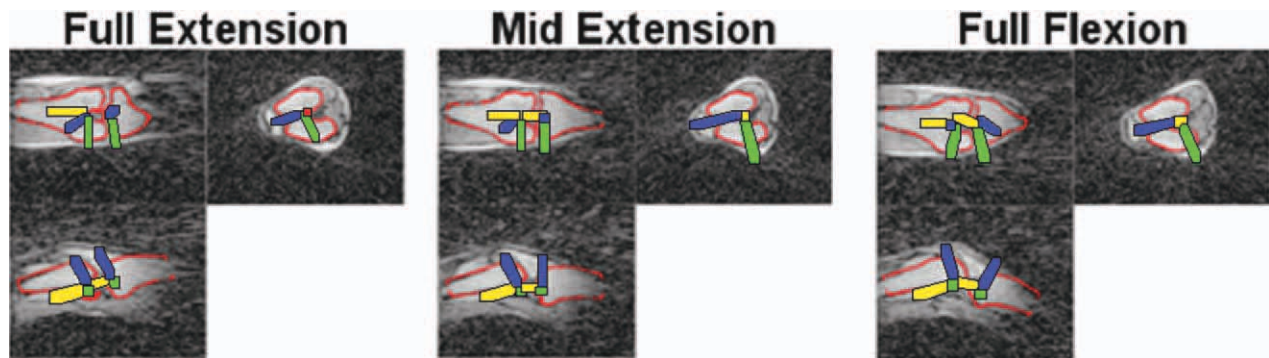

FIG. 5. Projections of the registered femur and tibia bone models (red lines) in the coronal (top left), axial (top right), and sagittal (bottom left) image planes for one subject at different knee flexion angles. Local reference frames for both the femur and the tibia are shown.
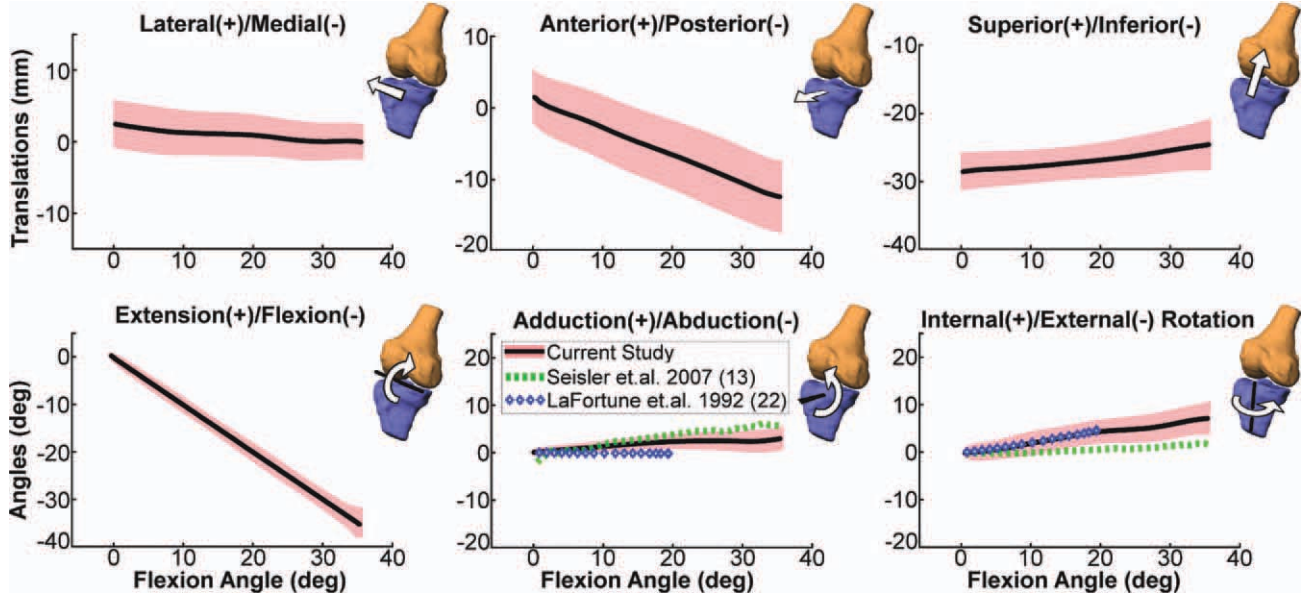
FIG. 6. Ensemble average tibiofemoral kinematics (shaded curves represent mean ± 1 standard deviation) for the dominant knee of 10 asymptomatic subjects over a flexion–extension motion cycle as measured using SPGR-VIPR. For comparison, the average adduction and rotation angle data measured by cine-PC MRI during unloaded knee flexion–extension (13) and via intracortical traction pins during normal gait (22) are shown. Our data show greater internal tibia rotation with knee flexion compared to cine PC, which may be related to greater quadriceps activation induced by our loading device (23).

assessment of skeletal position and orientation in three dimensions.

Previous studies have used cine phase-contrast (3) sequences to measure cyclic skeletal motion. However, Cartesian acquisition techniques used in these prior studies limited the number of imaging planes that could be acquired in reasonable scan times. For example, Seisler and Sheehan used a 2.75-min sequence to image a single plane of tibiofemoral motion with 1.2×1.8 mm^2 spatial resolution and 73.6 ms temporal resolution. We note that despite acquiring a single imaging plane, PC imaging does allow one to measure 3D velocities, which can be numerically integrated to estimate how 3D skeletal position and orientation evolve over time (9). A phantom study using cine PC reported average tracking errors of 0.33 mm for medial–lateral translation, 0.25 mm for anterior–posterior translation, and 0.9° for internal–external rotation (24). These errors may be attributable to numerical drift associated with integration. In addition, when cine-PC is used for in vivo imaging, there is potential for additional bias errors that arise from the inherent challenge of defining 3D anatomical reference frames by digitizing points in planar images (25).

The current standard for 3D dynamic imaging of in vivo skeletal motion is biplane fluoroscopy, which can be collected at high frame rates during functional tasks such as walking, running, and stair climbing (26–28). When tantalum beads are embedded in the bones, fluoroscopy data can be used to track skeletal translations with a precision of 0.12 mm (26). Model-based tracking using biplane fluoroscopy is slightly less accurate with reported errors of less than 1° and 0.7 mm at the knee (26). While the real-time imaging and low errors are impressive, fluoroscopy requires highly specialized set-ups,

exposes subjects to ionizing radiation, and does not directly provide soft tissue information. In contrast, dynamic MRI is promising due to its wide availability, safety, and capacity to simultaneously image soft tissue and bone morphology. These characteristics make dynamic MRI a potentially more viable option for clinical practice and longitudinal studies, in which one may wish to image skeletal motion at multiple time points to assess how joint mechanics adapt following musculoskeletal injuries, surgical treatment, and/or rehabilitation. Additional soft tissue information could also provide insight into cartilage contact and tendon/ligament deformation (29).

The VIPR acquisition in our technique offers some intrinsic advantages over standard Cartesian acquisitions. The radial undersampling allows for scan time reductions and for flexible retrospective gating while supporting relatively high spatial and temporal resolution. For comparison, a fully sampled Cartesian-based SPGR sequence with similar coverage and spatial and temporal resolution would require 102 ($160 \times 160 \times 60 \times 4$ ms) min compared to our current scan time of 5 min using SPGR-VIPR. With radial sampling and pseudorandom view ordering, data sorting can be accomplished retrospectively with offline reconstruction. This is not possible with a Cartesian acquisition that would require real-time prospective gating with a position feedback loop or dramatic oversampling of the required phase encodings.

In this study, we imaged knee kinematics for five consecutive minutes over 150 cycles of knee flexion/extension performed at 0.5 Hz. We assessed intercycle repeatability via external kinematic and kinetic measures, which showed the subjects exhibited relatively low variations in cycle times, knee range of motion and net
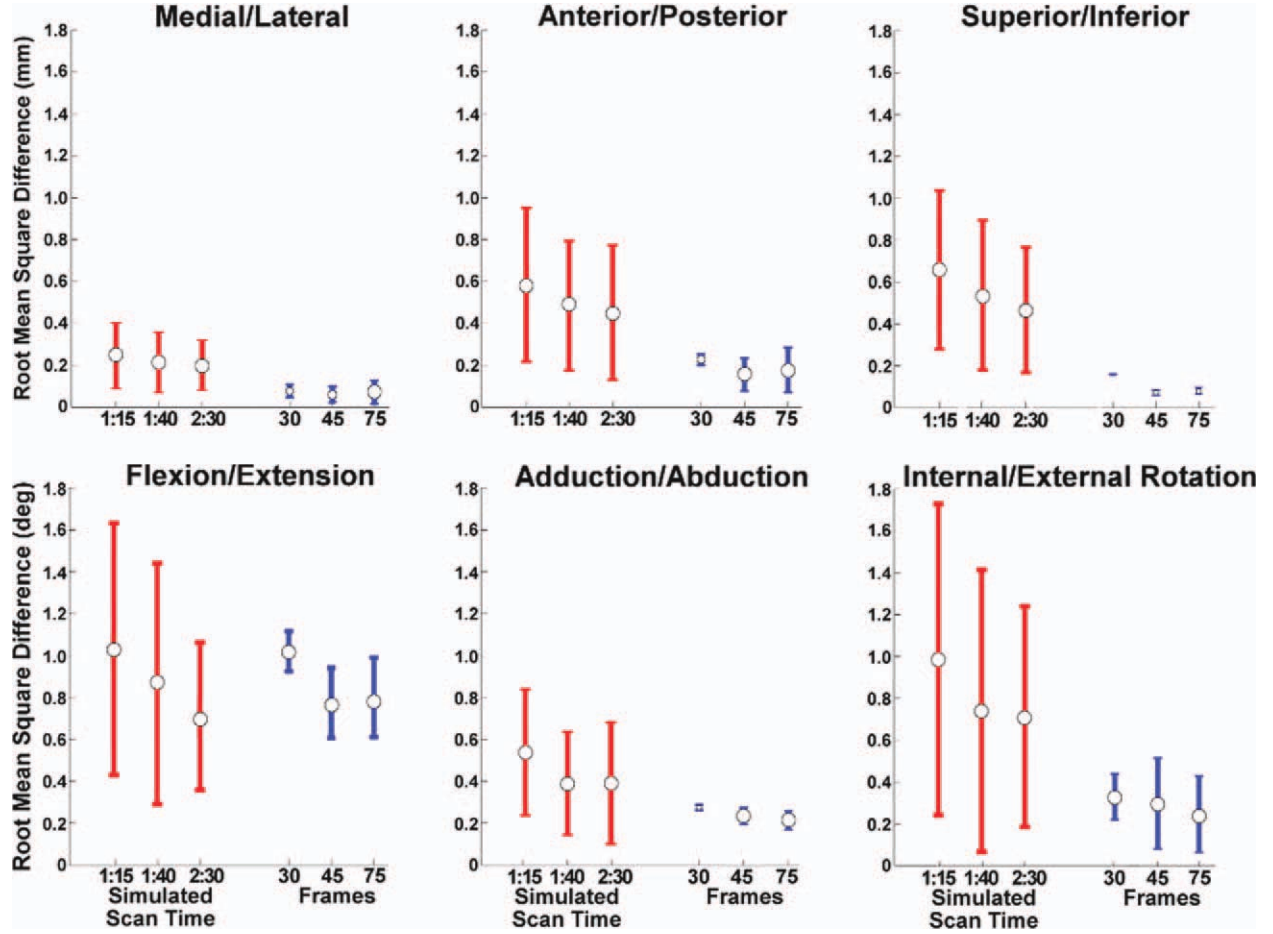
FIG. 7. Effects of scan time (for all subjects) and the number of reconstructed frames (three subjects) on tibiofemoral kinematics. The values shown are the average (±1 standard deviation) root-mean-squared difference in joint angles and translations, with respect to a 5:00 min scan reconstructed to 60 frames. Acceleration factors of 2–4 correspond to simulated scan times of 2:30, 1:40, and 1:15, respectively.

internal knee moments over the 150 repeat cycles (Fig. 4). The peak knee extension moment was ∼0.5 N m/kg, which is at the lower end of the magnitudes seen in the load acceptance phase of gait (17,30). Hence, the imaging task can be considered somewhat comparable to the quadriceps loads experienced during walking, and thus would not be considered overly fatiguing when performed for 5 min.

The measured nonsagittal knee angles agreed very well with knee motion measured using intracortical traction pins during gait (Ref. 22; Fig. 6). In particular, all knees exhibited internal tibia rotation with knee flexion (i.e., the screw-home mechanism; Ref. 31). We measured greater internal rotation than a prior cine PC study of the unloaded knee during flexion (Fig. 6). This difference could be attributed to the activation of quadriceps with knee flexion that was induced by our loading device (32), supporting the use of inertial loading to mimic functional knee loading seen in gait.

The sensitivity of the derived kinematics to scan time duration was sufficiently low, such that it may be feasible to reduce scan times to below 2 min without degrading the knee kinematic information obtained (Fig. 7). We note that the current results use a single channel flex

coil that was available at the time of the study. We expect that the higher signal-to-noise ratio achievable on multichannel flex coils could be used to either enhance image quality or further reduce scan time.

Our process uses a cine acquisition, which means that an average knee kinematic pattern is obtained, rather than a real-time assessment of each motion cycle. Hence, it would not be feasible to use the SPGR-VIPR approach to assess infrequent or nonrepeatable motion abnormalities. However, an assessment of normative kinematic patterns may be well relevant for understanding the link between chronic loading and the progression of joint disease. For example, early onset osteoarthritis is often seen within 10–15 years in patients who undergo surgical reconstruction of the anterior cruciate ligament (33). Recent literature suggests that abnormal joint kinematics can develop over time and may contribute to osteoarthritis development by inducing a chronic deviation from normative cartilage loading patterns (34). The dynamic MR imaging techniques illustrated here provide a potential mechanism by which to investigate this hypothesis by tracking longitudinal changes in tibiofemoral kinematics. In addition, it may be feasible to couple high-resolution bone and cartilage models together with the

kinematic data to quantitatively assess cartilage contact patterns (Fig. 1). A prior sensitivity study found that cartilage contact estimates based on proximity functions are highly dependent on the accuracy of the measured knee kinematics (35). To get a quantitative assessment of the sensitivity, we investigated how a 0.2-mm deviation in any of the three translational degrees of freedom would affect the estimated center of cartilage contact using bone/cartilage models from a subject in this study. This analysis showed that a 0.2-mm deviation induced up to a 1.2-mm change in center of contact location, with an average shift of 0.5 mm. Given this level of accuracy exceeds current dynamic MRI techniques (24), an important next step is to use a 3D motion phantom to assess absolute accuracy of kinematic measures obtained with SPGR-VIPR.

In summary, this article describes a novel dynamic volumetric imaging (SPGR-VIPR) approach to measure in vivo knee kinematics. Initial results are very promising, with good agreement seen between our image-based measures and kinematics measured using more invasive techniques during gait (13,22). Hence, dynamic volumetric imaging provides a potentially powerful approach to quantitatively characterize changes in skeletal joint mechanics that can arise with injury, pathology, and treatment.

ACKNOWLEDGMENTS

REFERENCES

1. Carpenter RD, Majumdar S, Ma CB. Magnetic resonance imaging of 3-dimensional in vivo tibiofemoral kinematics in anterior cruciate ligament-reconstructed knees. Arthroscopy 2009;25:760–766.
2. Gold GE. Dynamic and functional imaging of the musculoskeletal system. Semin Musculoskelet Radiol 2003;7:4.
3. Draper CE, Besier TF, Santos JM, Jennings F, Fredericson M, Gold GE, Beaupre GS, Delp SL. Using real-time MRI to quantify altered joint kinematics in subjects with patellofemoral pain and to evaluate the effects of a patellar brace or sleeve on joint motion. J Orthop Res 2009;27:571–577.
4. McNally EG, Ostlere SJ, Pal C, Phillips A, Reid H, Dodd C. Assessment of patellar maltracking using combined static and dynamic MRI. Eur Radiol 2000;10:1051–1055.
5. Tashman S, Kopf S, Fu FH. The kinematic basis of ACL reconstruction. Oper Tech Sports Med 2008;16:116–118.
6. Sheehan FT. The finite helical axis of the knee joint (a non-invasive in vivo study using fast-PC MRI). J Biomech 2007;40:1038–1047.
7. Sheehan FT. The 3D patellar tendon moment arm: quantified in vivo during volitional activity. J Biomech 2007;40:1968–1974.
8. Patel VV, Hall K, Ries M, Lotz J, Ozhinsky E, Lindsey C, Lu Y, Majumdar S. A three-dimensional MRI analysis of knee kinematics. J Orthop Res 2004;22:283–292.
9. Sheehan FT, Zajac FE, Drace JE. Using cine phase contrast magnetic resonance imaging to non-invasively study in vivo knee dynamics. J Biomech 1998;31:21–26.
10. d'Entremont A, Nordmeyer-Massner J, Bos C, Wilson D, Pruessmann K. A dynamic measurement method for knee biomechanics. In: Proceedings of the 19th Annual Meeting of ISMRM, Montreal, Canada, 2011.
11. Draper CE, Santos JM, Kourtis LC, Besier TF, Fredericson M, Beaupre GS, Gold GE, Delp SL. Feasibility of using real-time MRI to measure joint kinematics in 1.5T and open-bore 0.5T systems. J Magn Reson Imaging 2008;28:158–166.
12. Zhu Y, Drangova M, Pelc N. Fourier tracking of myocardial motion using cine PC data. Magn Reson Med 1996;35:471–480.
13. Seisler AR, Sheehan FT. Normative three-dimensional patellofemoral and tibiofemoral kinematics: a dynamic, in vivo study. IEEE Trans Biomed Eng 2007;54:1333–1341.
14. Johnson KM, Lum DP, Turski PA, Block WF, Mistretta CA, Wieben O. Improved 3D phase contrast MRI with off-resonance corrected dual echo VIPR. Magn Reson Med 2008;60:1329–1336.
15. Silder A, Westphal CJ, Thelen DG. A magnetic resonance-compatible loading device for dynamically imaging shortening and lengthening muscle contraction mechanics. J Med Dev 2009;3: 034504-1–034504-5.
16. Winter D, Yack H. EMG profiles during normal human walking: stride-to-stride and inter-subject variability. Electroencephalogr Clin Neurophysiol 1987;67:402–411.
17. Besier TF, Fredericson M, Gold GE, Beaupre GS, Delp SL. Knee muscle forces during walking and running in patellofemoral pain patients and pain-free controls. J Biomech 2009;42:898–905.
18. Miranda DL, Rainbow MJ, Leventhal EL, Crisco JJ, Fleming BC. Automatic determination of anatomical coordinate systems for three-dimensional bone models of the isolated human knee. J Biomech 2010;43:1623–1626.
19. Pruessmann KP, Weiger M, Börnert P, Boesiger P. Advances in sensitivity encoding with arbitrary k-space trajectories. Magn Reson Med 2001;46:638–651.
20. Powell MJD. An efficient method for finding the minimum of a function of several variables without calculating derivatives. Comput J 1964;7:155–162.
21. Grood E, Suntay W. A joint coordinate system for the clinical description of three-dimensional motions: application to the knee. J Biomech Eng 1983;105:136–144.
22. Lafortune M, Cavanagh P, Sommer H, Kalenak A. Three-dimensional kinematics of the human knee during walking. J Biomech 1992;25: 347–357.
23. Li G, Rudy T, Sakane M, Kanamori A, Ma C, Woo SLY. The importance of quadriceps and hamstring muscle loading on knee kinematics and in-situ forces in the ACL. J Biomech 1999;32:395–400.
24. Behnam AJ, Herzka DA, Sheehan FT. Assessing the accuracy and precision of musculoskeletal motion tracking using cine-PC MRI on a 3.0T platform. J Biomech 2011;44:193–197.
25. Morton NA, Maletsky LP, Pal S, Laz PJ. Effect of variability in anatomical landmark location on knee kinematic description. J Orthop Res 2007;25:1221–1230.
26. Anderst W, Zauel R, Bishop J, Demps E, Tashman S. Validation of three-dimensional model-based tibio-femoral tracking during running. Med Eng Phys 2009;31:10–16.
27. Tashman S. Abnormal rotational knee motion during running after anterior cruciate ligament reconstruction. Am J Sports Med 2004;32: 975–983.
28. Li G, Kozanek M, Hosseini A, Liu F, Van de Velde SK, Rubash HE. New fluoroscopic imaging technique for investigation of 6DOF knee kinematics during treadmill gait. J Orthop Surg Res 2009;4:1–5.
29. Sheehan FT, Drace JE. Human patellar tendon strain: a noninvasive, in vivo study. Clin Orthop Relat Res 2000;370:201–207.
30. Whittington B, Silder A, Heiderscheit B, Thelen DG. The contribution of passive-elastic mechanisms to lower extremity joint kinetics during human walking. Gait Posture 2008;27:628–634.
31. Hallen L. The 'screw-home' movement in the knee joint. Acta Orthop Scand 1966;37:97–106.
32. Victor J, Labey L, Wong P, Innocenti B, Bellemans J. The influence of muscle load on tibiofemoral knee kinematics. J Orthop Res 2010; 28:419–428.
33. Lohmander LS, Englund PM, Dahl LL, Roos EM. The long-term consequence of anterior cruciate ligament and meniscus injuries: osteoarthritis. Am J Sports Med 2007;35:1756–1769.
34. Tashman S, Kolowich P, Collon D, Anderson K, Anderst W. Dynamic function of the ACL-reconstructed knee during running. Clin Orthop Relat Res 2007;454:66–73.
35. Yao J, Salo AD, Lee J, Lerner AL. Sensitivity of tibio-menisco-femoral joint contact behavior to variations in knee kinematics. J Biomech 2008;41:390–398.